NEURAL REGENERATION RESEARCH
Volume 8, Issue 31, November 2013

www.nrronline.org

doi:10.3969/j.issn.1673-5374.2013.31.007 [http://www.nrronline.org; http://www.sjzsyj.org]
Yang YJ, Gao LY, Fu J, Zhang J, Li YX, Yin B, Chen WJ, Geng DY. Apparent diffusion coefficient evaluation for secondary changes in the cerebellum of rats after middle cerebral artery occlusion. Neural Regen Res. 2013;8(31):2942-2950.

Apparent diffusion coefficient evaluation for secondary changes in the cerebellum of rats after middle cerebral artery occlusion

Yunjun Yang[1], Lingyun Gao[2], Jun Fu[2], Jun Zhang[1], Yuxin Li[1], Bo Yin[1], Weijian Chen[2], Daoying Geng[1]

1 *Department of Radiology, Huashan Hospital, Fudan University, Shanghai 200040, China*
2 *Department of Radiology, First Affiliated Hospital of Wenzhou Medical University, Wenzhou 325000, Zhejiang Province, China*

Graphical Abstract

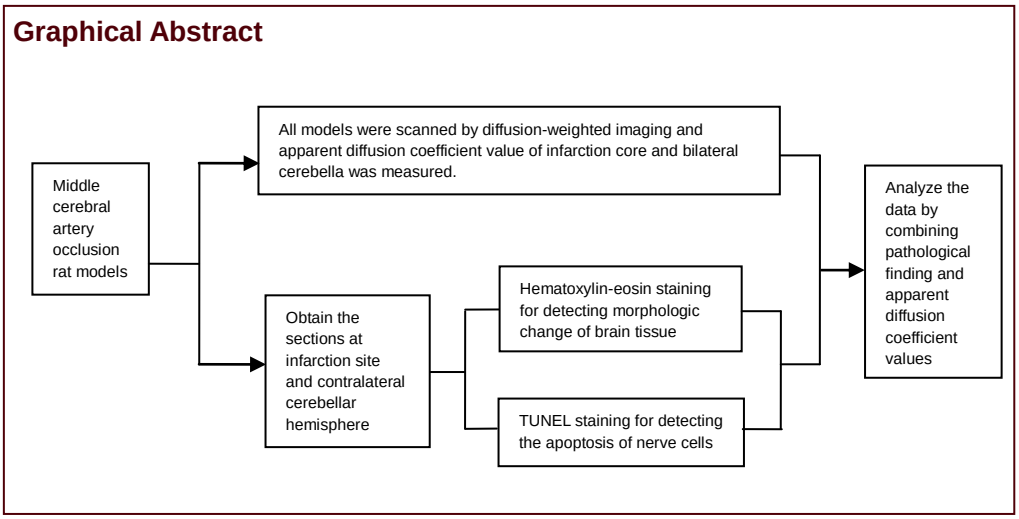

Abstract

Supratentorial cerebral infarction can cause functional inhibition of remote regions such as the cerebellum, which may be relevant to diaschisis. This phenomenon is often analyzed using positron emission tomography and single photon emission CT. However, these methods are expensive and radioactive. Thus, the present study quantified the changes of infarction core and remote regions after unilateral middle cerebral artery occlusion using apparent diffusion coefficient values. Diffusion-weighted imaging showed that the area of infarction core gradually increased to involve the cerebral cortex with increasing infarction time. Diffusion weighted imaging signals were initially increased and then stabilized by 24 hours. With increasing infarction time, the apparent diffusion coefficient value in the infarction core and remote bilateral cerebellum both gradually decreased, and then slightly increased 3–24 hours after infarction. Apparent diffusion coefficient values at mote regions (cerebellum) varied along with the change of supratentorial infarction core, suggesting that the phenomenon of diaschisis existed at the remote regions. Thus, apparent diffusion coefficient values and diffusion weighted imaging can be used to detect early diaschisis.

Key Words

neural regeneration; brain injury; cerebral ischemia; cerebral infarction; magnetic resonance imaging; apparent diffusion coefficient; middle cerebral artery occlusion; diffusion weighted imaging; infarction core; remote regions; diaschisis; grants-supported paper; neuroregeneration

Yunjun Yang, Ph.D., Associate professor.

Yunjun Yang and Lingyun Gao contributed equally to this work.

Corresponding author: Daoying Geng, Professor, Department of Radiology, Huashan Hospital, Fudan University, Shanghai 200040, China, wzmcyyunjun@163.com.

Received: 2013-07-20
Accepted: 2013-10-05
(N201306040)

Acknowledgments: We thank the postgraduates Wang S, Tong QY, Wu N and Lin Y from the First Affiliated Hospital of Wenzhou Medical College in China for MRI scans.

Funding: This study was supported by Zhejiang Province Science and Technology Plan Project in China, No. 2012C37029; Public Welfare Technology Application Research Plan Project of Zhejiang Province in China, No. 2011C23021.

Author contributions: Yang YJ and Chen WJ were in charge of manuscript authorization, and provided technical or material support. Geng DY and Chen WJ obtained the funding and served as principle investigators. Gao LY, Fu J, Zhang J, Li YX participated in establishing the models, provided experimental data and ensured the integrity of the data. Gao LY, Zhang J and Yin B participated in data analysis. Yang YJ and Gao LY wrote the manuscript. Fu J was responsible for data arrangement. Geng DY and Yang YJ were responsible for modifying and polishing the paper. All authors approved the final version of the paper.

Conflicts of interest: None declared.

Ethical approval: This study was approved by the Ethics Committee, the First Affiliated Hospital of Wenzhou Medical College, China.

Author statements: The manuscript is original, has not been submitted to or is not under consideration by another publication, has not been previously published in any language or any form, including electronic, and contains no disclosure of confidential information or authorship/patent application/finding source disputations.

INTRODUCTION

Most previous studies have detected the phenomenon of diaschisis using positron emission tomography[1-3], single photon emission CT[4-5] or perfusion weighted imaging[6-8]. However, positron emission tomography/single photon emission CT often require a radioactive tracer material to be injected into the body, and a γ-photon detector then indirectly observes the distribution of the compound and specifically reflects the changes of blood flow, as well as function and metabolism, in organs or lesions. In addition, these tracer materials have characteristic short half-lives and radioactivity, and the examination often requires equipment preparation in a short time windows. Therefore, compared with CT and MRI, positron emission tomography/single photon emission CT is more expensive and more radioactive (as the radioactive material is directly injected into body). At present, diffusion weighted imaging (DWI) is the only functional non-invasive MRI method available to quantify the diffusion status of water molecule in living tissue[9-11]. Furthermore, apparent diffusion coefficient (ADC), which eliminates T2 from DWI, can more objectively quantize dispersion movement of tissue water molecules[12-13].

We suggested that if DWI findings associated with hematoxylin-eosin staining under light microscope and immunohistochemical methods show no changes in remote brain regions (such as the cerebellum) after middle cerebral artery occlusion (MCAO), which illustrate that remote brain regions are not affected (*i.e.*, without diaschisis). However, it has also been suggested that DWI and ADC values cannot determine diaschisis. Nevertheless, if changes in ADC values are found in the cerebellum after MCAO, while light microscope and immunohistochemical results show apoptotic cells, which illustrate that cerebral infarction after left MCAO injures the cerebellum. If changes in ADC values are found in the cerebellum after MCAO while light microscope and immunohistochemical results show no apoptotic cells, which illustrate that the cerebellum has no substantial injury. This is because cerebral infarction after left MCAO indirectly leads to secondary lesion of the cerebellum *via* nerve conduction pathways, which is termed diaschisis.

Therefore, in our study, we applied the ADC of DWI in combination with the light microscopy examination of hematoxylin-eosin staining and immunohistochemistry for detecting apoptotic cells and secondary changes in the cerebellum following MCAO.

RESULTS

Quantitative analysis of experimental animals

Thirty-five rats were randomly assigned into the model group (n = 28) and the normal control group (n = 7). The rats in the model group, which involved ligation of the external carotid artery to establish the MCAO models, were divided into 1-, 3-, 9-, and 24-hour subgroups according to the time of sampling. During the MCAO modeling process, three rats died because of anesthesia accidents, and two rats died because of the sensitivity of traction vagus. Fourteen rats in the 1-hour and 3-hour subgroups all survived after MCAO; one rat in the 9-hour group and two in the 24-hour group died. The remaining rats successfully completed the MRI examination, and data of the dead animals were supplemented during further experiments and added into final experimental data.

MRI manifestation of brain tissue of MCAO rats

T2-weighted imaging and DWI showed no differences in ADC values of the left basal ganglia and bilateral cerebella at different time points in the control group (P > 0.05). As the infarction time extended, DWI showed that the infarction area of the left basal ganglia (infarction core) increased gradually to involve the cerebral cortex (Figure 1), and the DWI signals were also increased. However, T2-weighted imaging and the DWI signal in the bilateral cerebellum remained unchanged (Figure 2).

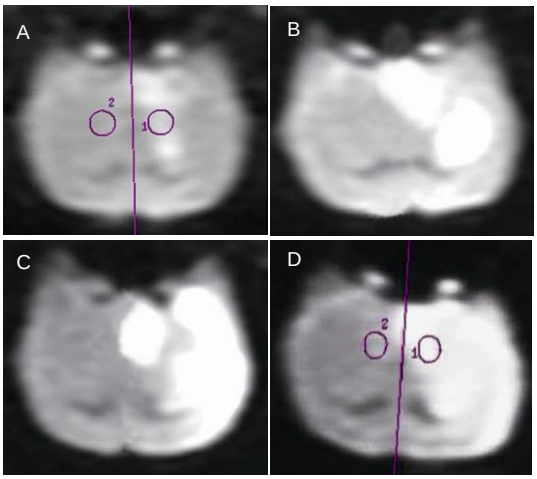

Figure 1 Sequential MRI manifestation of infarction core of middle cerebral artery occlusion rats (diffusion weighted imaging).

(A–D) In the 1-, 3-, 9-, and 24-hour subgroups after middle cerebral artery occlusion, the infarction area of the left basal ganglia (left high signal) increased gradually as the infarction progressed, and involved the cerebral cortex. Numbers 1 and 2 in figures represent the region of interest of symmetrical parts in the bilateral cerebrum.

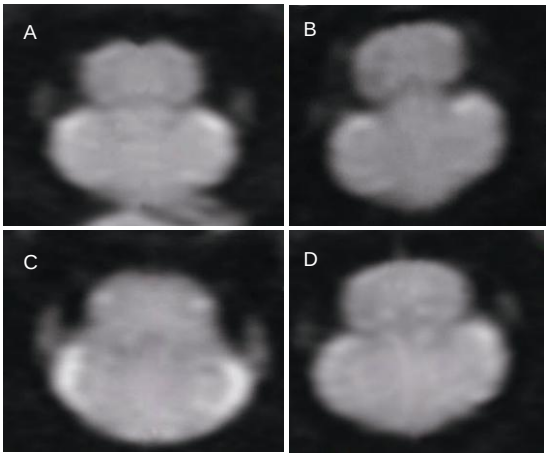

Figure 2 Sequential MRI manifestation of the bilateral cerebella of middle cerebral artery occlusion rats (diffusion weighted imaging).

(A–D) In the 1-, 3-, 9-, and 24-hour subgroups after middle cerebral artery occlusion, there were no obvious signal abnormalities in the bilateral cerebella.

The ADC value at the infarction core and cerebellum was decreased (P < 0.01) at 1 hour after infarction. Compared with the normal control group, the ADC value at the infarction core was decreased by approximately 58% (P < 0.05), and the decrease in the right cerebellum (24%, P < 0.05) was higher than that of the left cerebellum (20%, P < 0.05). With increasing infarction time, the ADC value of the infarction core showed no apparent changes (Figure 3, Table 1).

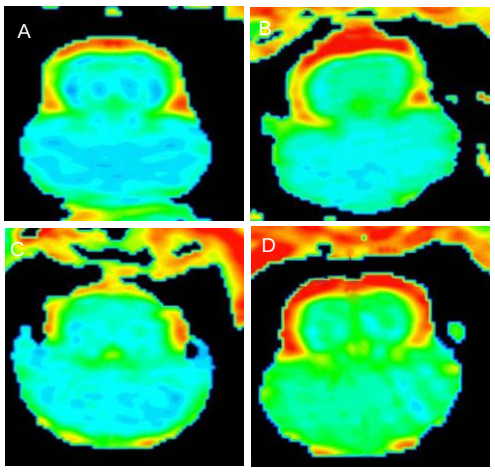

Figure 3 Apparent diffusion coefficient maps of the cerebellum of middle cerebral artery occlusion rats.

(A–D) In the 1-, 3-, 9-, and 24-hour subgroups after middle cerebral artery occlusion, the cerebellar signal was the lowest (blue) at 1 hour. With increasing infarction time, cerebellar signal gradually increased (yellow-green).

Histopathological changes in brain tissue of MCAO rats

In the normal control and model groups, hematoxylin-eosin staining showed evidence of large and round neuronal nuclei, located in the center of the cells in the bilateral cerebella. The cytoplasm of cells was abundant, with no obvious abnormalities. At 1 hour after MCAO, neurons in the infarct area showed no abnormalities by light microscope, but individual neurons showed nuclear hyperchromatism and cytoplasm acidophily alterations. At 3 hours after MCAO, a small number of neurons showed nuclear hyperchromatism and cytoplasm eosinophilic alterations in the infarction area. At 9 hours after MCAO, the number of neurons exhibiting nuclear karyopyknosis with pyknosis further increased in the left hemisphere. At 24 hours after MCAO, more ischemic neurons with nuclear karyopyknosis were seen in the cerebral infarction region, and in some regions the nucleus of the neurons had disappeared and the number of neurons was reduced. By contrast, the size and quantity of neurons in the bilateral cerebellum showed no abnormality by light microscope over 1–24 hours (Figure 4).

Apoptotic cell death in brain tissue of MCAO rats

TUNEL staining showed that control rats exhibited normal brain cell numbers and morphology. With increasing MCAO time, the number of apoptotic cells in the infarction core gradually increased (2.40 ± 0.55/200 × field of view at 1 hour after MCAO, 6.40 ± 1.67/200 × field of view at 3 hours after MCAO, 37.40 ± 5.73/200 × field of view at 9 hours after MCAO, and 61.00 ± 7.48/200 × field of view at 24 hours after MCAO), while no apoptotic cells were observed in the cerebellum at any time point (Figure 5).

Table 1 Changes in apparent diffusion coefficient (ADC) values in the infarction core and the cerebella at 1–24 hours after middle cerebral artery occlusion (× 10^{-4}/mm^2)

Location	Normal control group	Time after middle cerebral artery occlusion group (hour)			
		1	3	9	24
Left basal ganglia (infarction core)	8.226±0.277	3.418±1.197[a]	3.242±0.065[a]	3.175±0.481[a]	3.732±1.348[a]
Right cerebellum	7.480±0.253	5.668±0.339[a]	6.802±0.047[a]	6.430±0.240[a]	6.578±0.286[a]
Left cerebellum	7.317±0.163	5.850±0.101[a]	6.410±0.585	6.198±0.136[a]	6.632±0.292[a]

Data are expressed as mean ± SD. There were seven rats in each group. The comparisons of ADC values in the normal control group were performed by paired *t*-test. The comparisons of ADC values in the two groups or various locations were performed by repeated-measures analysis of variance. [a]*P* < 0.01, *vs*. normal control group.

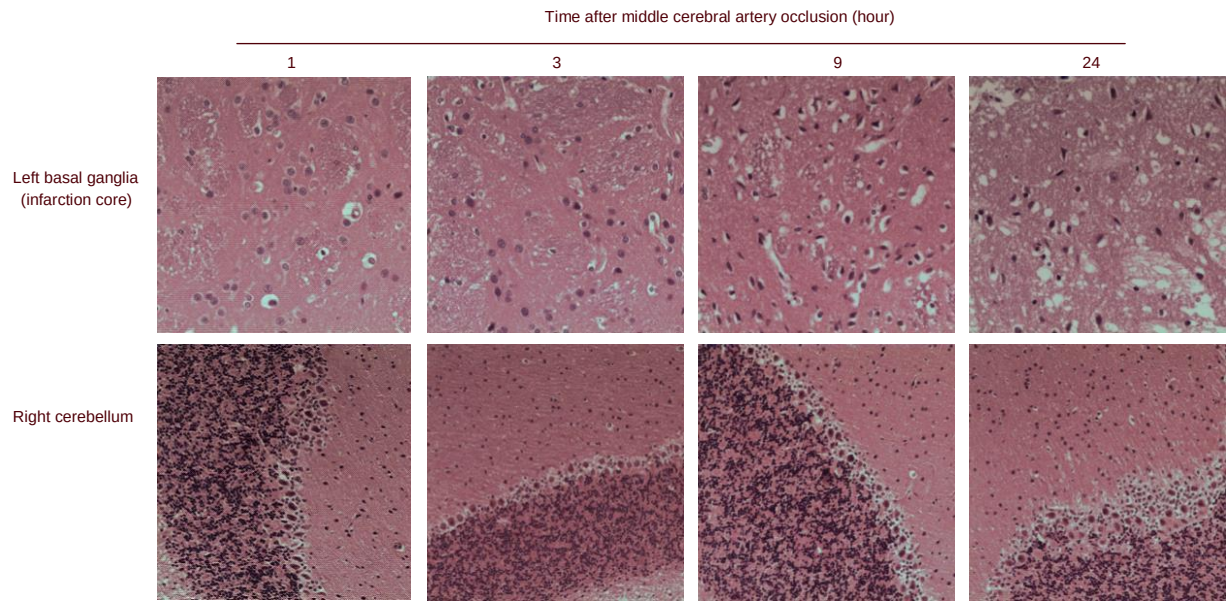

Figure 4 Histopathological changes in brain tissue of middle cerebral artery occlusion rats (hematoxylin-eosin staining, × 200).

With increasing occlusion time, there was progressive worsening of secondary neuronal damage in the cerebral infarction area. By contrast, the morphology of cerebellar nerve cells was normal.

DISCUSSION

In our study, DWI showed a high signal area at the infarction core area at 1 hour after MCAO model establishment. With increasing time of MCAO time, the signal became larger and higher, and the boundary was clearer. The statistical analysis for the changes in ADC value with time at the infarction core area showed that ADC values rapidly decreased at 1 hour after MCAO, slowly decrease at 3–9 hours, and then constantly increased during 9–24 hours, although still remained below normal levels. The changes in ADC values at the infarction core were associated with cytotoxic edema[14] and vasogenic edema[15]. The cells at the infarction core area remain hypertonic so that extracellular water enters into the cells and the extracellular space becomes smaller, while the total tissue water content remains constant[16]. With the influence of the barrier of cell membrane and organelles, as well as the absorption of macromolecular proteins, the diffusion movements of a large proportion of intracellular water is restricted, which leads to decreasing ADC values and high signal on DWI. With the presence of progressive infarction, the collateral circulation does not compensate fully. Further, the prolonged swelling of cells induces ischemia, necrosis and gradual cellular disintegration, injury to vascular endothelial cells, damage to the blood-brain barrier, and a large amount of water and protein release from the capillary bed to the extracellular space, resulting in enlargement of the extracellular space and an increase of free water[16]. Accordingly, the ADC values began to rise and the DWI signals decreased. When edema is aggravated, the overall diffusion of water molecules accelerates, resulting in a gradual increase in ADC values close to the normal level.

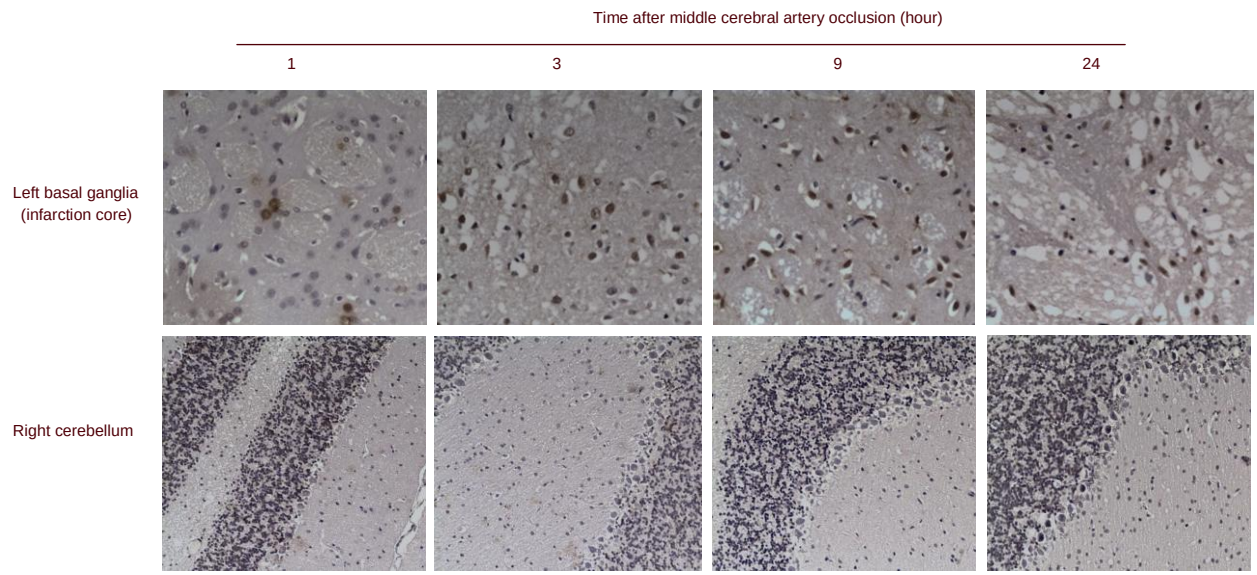

Figure 5 Histopathological changes in brain tissue of middle cerebral artery occlusion rats (TUNEL staining, × 200).

With increasing occlusion time, there was a progressive increase in the number of apoptotic cells in the cerebral infarction site. By contrast, there was no evidence of apoptosis of cerebellar nerve cells.

When DWI is applied to evaluate hyperacute and acute supratentorial cerebral infarction, most studies have examined the lesion itself and changes of the surrounding ischemic penumbra[17-23], rather than examining the signal changes at remote locations such as the cerebellum. Importantly, the results of the present study indicated that the ADC values of the cerebellum changed with the development of the infarct core. Nevertheless, unlike the finding that the number of apoptotic cells at the supratentorial infarction core increased with time, no cerebellar cells were apoptotic during the 24 hours. The reason for this phenomenon may be that the nerve signal transmission originating from the fronto-parietal cortex is affected after pathological changes in neurons in the supratentorial infarction core. With the crossing nerve fibers connecting between the bilateral cerebellums, the nerve signals lead to functional inhibition of the remote cerebellum, but without pathological changes. In the present study, the ADC values were statistically different between the bilateral cerebellums after supratentorial cerebral infarction compared with those in the normal control group, indicating that supratentorial infarction brain tissue in MCAO models can affect normal signal transduction of the cortico-ponto-cerebellar neural fiber pathway[24-27]. These changes in neural activity can result in altered coupling of local blood flow[28]. The ADC value within tissues can reflect water molecular diffusion and capillary perfusion[29]. As such, cerebellar ADC values exhibited differences after supratentorial cerebral infarction, including contralateral (right) cerebellar diaschisis and ipsilateral (left) cerebellar diaschisis. At the same time the ADC values of the cerebellum exhibited fluctuating changes, with a mild decrease at 9 hours after infarction. The ADC values at the right cerebellum changed more than the left hemisphere, then they both decreased. The reason for these phenomena may be related to the following factors. After ischemia and hypoxia in the early phase of left MCAO, the brain tissue is compensated by the increasing blood flow and the cytotoxic edema is mitigated, and ADC values of remote controlled regions are recovered. With increasing degree of infarction, the brain tissue cannot compensate for reductions in local blood supply, resulting in neuronal necrosis. Thus, the ADC values had a slight fluctuation at 9 hours, but the variation was mild. The ADC values of the right cerebellum decreased more apparently than the left at 1 hour after infarction. This may be because the corticospinal tract nerve fibers from the frontal and parietal cortex mostly cross to the contralateral cerebellum, but only a small part of these pathways entered the ipsilateral cerebellum. Thus, left cerebral hemisphere infarction caused more severe effects on the right cerebellar hemisphere.

The changes in ADC values of distant brain structures after MCAO are consistent with the diaschisis theory[1, 4, 6, 30]. Diaschisis is a clinical symptom that commonly appears after ischemic infarction, but which does not match the imaging examination of the infarction. Diaschisis involves the process whereby local brain damage leads to tran-

sient functional inhibition of normal structures at remote regions that exhibit fiber connections to the primary lesion area. Diaschisis can be roughly divided into the following types[31]: ipsilateral hemisphere diaschisis; cerebellar diaschisis; thalamic diaschisis; and brainstem diaschisis. Diaschisis has the following features[32]: (1) it is the result of local brain damage; (2) it occurs at regions remote from the area of injury; (3) it involves functional inhibition of distant brain locations; (4) it involves corresponding neuronal fiber pathways; and (5) it is a reversible process and can be recovered over a certain period of time. In our study, we discovered cerebellar diaschisis following ischemic infarction in the rat brain. The contralateral cerebellar diaschisis (crossed cerebellar diaschisis) was more obvious than ipsilateral cerebellar diaschisis after supratentorial cerebral infarction, suggesting that crossed cerebellar diaschisis is potentially important. In 1980, Baron *et al* [4] first reported evidence of a decrease in contralateral cerebellar hemispheric blood flow and oxygen metabolism in patients with cerebral infarction by noninvasive 150 continuous inhalation method combined with positron emission tomography. In 1993, Sakashita *et al* [1] found 11 cases (nearly 78.6%) of hypoperfusion on the contralateral cerebellar hemisphere in 14 cases of supratentorial unilateral infarction using single photon emission CT. In 2009, Lin *et al* [6] analyzed magnetic resonance perfusion weighted images of 301 patients with cerebral infarction and found 47 patients with diaschisis. Similar experimental studies by Chu *et al* [30] also found diaschisis in the contralateral cerebellar hemisphere using hydrogen clearance in an MCAO model with cerebral infarction. Based on these findings, the results of our study were consistent with cerebellar diaschisis.

The study of diaschisis is often limited to positron emission tomography, single photon emission CT and other traditional methods. The ^{133}Xe inhalation method for measuring cerebral blood flow at remote sites has also been applied to explore clinical diaschisis phenomena[33]. Subsequently, positron emission tomography was used to report diaschisis by detecting the cerebral metabolic rate of oxygen[34] and cerebral metabolic rate of glucose[35]. Nagasawa and Kogure[36] also reported changes of distant sites after ischemia with ^{45}Ca autoradiography technology in a model of transient focal ischemia induced by embolization of the right middle cerebral artery. Further, Izumi *et al* [37] explored the changes in T2-weighted imaging in different brain regions after MCAO, which indirectly reflected the changes in remote brain regions. The role and connection between injury and remote regions was also examined in terms of hemodynamics using perfusion weighted imaging[38-39]. However, it is important to note that different imaging methods can produce differing results. For example, Madai *et al* [40] reported that positron emission tomography was more sensitive to detect cerebellar diaschisis than perfusion weighted imaging using 1.5T MRI. Jeon *et al* [41] analyzed 81 cases of acute cerebral infarction patients using multi-slice computed tomography, and evaluated the changes of cerebral blood flow, cerebral blood flow volume, mean transit time, and time to peak. Their results indicated that computed tomography perfusion imaging was a valid tool for the diagnosis of crossed cerebellar diaschisis in patients. Our study also suggested evidence of cerebellar diaschisis using changes in ADC values after MCAO.

In summary, we observed changes in ADC values in the cerebellum following an infarct core area in rodent MCAO models. These data demonstrate that diaschisis exists on both sides of the remote cerebellum, which was closely related to the nerve pathway from the site of infarction. Previous imaging evaluation of distant parts after supratentorial cerebral infarction are primarily limited to single photon emission CT, positron emission tomography, and perfusion weighted imaging. DWI is a routine sequence of clinical diagnosis of cerebral infraction that uses a high scanning speed without intravenous administration of contrast agents. Thus, DWI provides a convenient and efficient new method to evaluate diaschisis.

MATERIALS AND METHODS

Design

A randomized controlled animal experiment of neuroimaging.

Time and setting

The experiment was performed at the Clinical Centre of the First Affiliated Hospital of Wenzhou Medical College between December 2010 and March 2011.

Materials

Thirty-five adult male Sprague-Dawley rats, weighing 260–300 g, were provided by the Experimental Animal Center of Wenzhou Medical College, China (license No. SYXK (Zhe) 2010-0150). The rats were fed with standard feed and had free access to water in a quiet room at 20–25°C and 70% humidity. Animal experiments were performed in accordance with the *Guidance Suggestions for the Care and Use of Laboratory Animals*, issued by

the Ministry of Science and Technology of China[42].

Methods

Establishing MCAO model

The left MCAO model was prepared according to Longa's method[43]. We separated and exposed the common carotid artery, internal carotid artery, and external carotid artery, and then ligated the external carotid artery and its branches. A thread was inserted into the proximal part of common carotid artery. A small incision was then made close to the common carotid artery crotch, and a nylon suture inserted 18.5 ± 0.5 mm into the internal carotid artery and past the middle cerebral artery origin, to reach the proximal segment of the anterior cerebral artery. At this point, the intraluminal suture blocked the origin of the middle cerebral artery. The room temperature was maintained at 22°C, and each successful MCAO model was kept in a single cage.

MRI detection

Before MRI examination, the animals were anaesthetized with two intraperitoneal injections of 10% chloral hydrate. Two groups of experimental animals were examined by MRI at 1, 3, 9, and 24 hours after modeling. MRI was performed using a 3.0-T GE (GE, Medical System, Milwaukee, WI, USA) scanner with single-channel birdcage coil, including conventional T1-weighted imaging, T2-weighted imaging, and DWI. The sequence parameters were as follows: sequence scanning 10 layers, thickness 2.4 mm, and zero-gap scanning. For T1-weighted imaging: fast spin echo sequence, time of repetition/time of echo = 2 000/13.1 ms, field of view 6.0, number of excitations = 8.00, matrix 64 × 64. For T2-weighted imaging: fast spin echo sequence, time of repetition/time of echo = 2 000/24.2 ms, field of view 6.0, number of excitations = 8.00, matrix 64 × 64. For DWI: spin echo, single-shot echo-planar imaging sequences, time of repetition/time of echo = 2 000/80.4 ms, field of view 6.0, matrix 64 × 64, diffusion gradient in mutually perpendicular X, Y, Z axis, two diffusion sensitivity coefficients b = 0 s/mm^2 and b = 1 000 s/mm^2, ramp sampling, and imaging acquisition time 64 seconds. Quantitative ADC maps were generated using dedicated commercially available software (Functool 2; GE Healthcare). Two senior magnetic resonance physicians compared and analyzed the ADC maps and then measured ADC value of the 2-mm^2 region of interest.

Harvesting specimens

After MRI scan was completed, rats were euthanized by overdose of anesthesia. We cut a 1-mm-thick area of each of the infarction and cerebellum according to MRI scanning levels. After paraffin embedding, we cut consecutive coronal sections (5 mm thick). The sections were placed in 60°C oven for 30 minutes after mounting, and then stored in a slice box at room temperature.

Hematoxylin-eosin staining for detecting pathological change of brain tissue and cerebellum

Seven rats in each group (control group, MCAO 1-hour, 3-hour, 9-hour, and 24-hour groups) were collected, and two sections of the infarction core and contralateral cerebellum were selected for hematoxylin-eosin staining. Briefly, sections were dewaxed and rehydrated, rinsed in distilled water for 5 minutes, and then immersed in Mayer's hematoxylin for 5–10 minutes followed by rinsing for additional 5 minutes. The slices were then differentiated in 1% hydrochloric acid ethanol for 30 seconds, rinsed for 3 minutes to blue, and then immersed in eosin for 5 minutes, rinsed for 5 minutes, cleared, and mounted. We observed the pathological change using light microscopy (Olympus, Tokyo, Japan).

TUNEL staining for detecting the apoptosis of nerve cells

Brain tissue sections of rats in each group were dewaxed and incubated with hydrogen peroxide, rinsed, incubated in Proteinase K, rinsed with PBS, incubated in TUNEL reaction mixture (Boehringer Mannheim, Beijing, China), rinsed with PBS, blocked with hydrogen peroxide methanol and sheep serum, incubated in transforming agent-peroxidase, rinsed with PBS, developed with DAB, rinsed with water, counter-stained in Mayer's hematoxylin, rinsed with water, differentiated in hydrochloric acid alcohol, rinsed, cleared, and mounted. Every section was counted manually in five high-power fields (200 × magnification). Finally, we calculated the average number of the TUNEL-positive cells.

Statistical analysis

Data were statistically analyzed using SPSS 16.0 software (SPSS, Chicago, IL, USA) and the results were expressed as mean ± SD. The comparisons of ADC values in the normal control group were performed by paired t-test. ADC values in various locations and apoptotic cells (TUNEL-positive cells) at different time points were compared using repeated measures analysis of variance. A P value < 0.05 was considered statistically significant.

Research background: Ischemic cerebrovascular disease can cause functional inhibition of remote regions (*e.g.*, the cerebellum), which may be relevant to diaschisis.

Research frontiers: Previous studies have focused on changes

in magnetic resonance diffusion-weighted imaging and apparent diffusion coefficient values in ischemic cerebrovascular disease lesions and the surrounding ischemic penumbra. However, the secondary changes in the cerebellum after supratentorial unilateral cerebral ischemic infarction are largely unknown.

Clinical significance: Apparent diffusion coefficient values can effectively detect and quantify changes in remote regions after supratentorial unilateral cerebral infarction, thus providing a new method for clinical evaluation of diaschisis after cerebral infarction.

Academic terminology: Diaschisis is the phenomenon where local brain damage can lead to transient functional inhibition of normal structures at remote regions that have neural fiber connections to the primary lesion.

Peer review: Apparent diffusion coefficient values were examined to explain the apoptosis of cerebellar nerve cells after unilateral middle cerebral artery occlusion. The analysis of pathological findings increased the strength of the paper.

REFERENCES

[1] Sakashita Y, Matsuda H, Kakuda K, et al. Hypoperfusion and vasoreactivity in the thalamus and cerebellum after stroke. Stroke. 1993;24(1):84-87.

[2] Nocuń A, Wojczal J, Szczepańska-Szerej H, et al. Quantitative evaluation of crossed cerebellar diaschisis, using voxel-based analysis of Tc-99m ECD brain SPECT. Nucl Med Rev Cent East Eur. 2013;16(1):31-34.

[3] Kurisu K, Kawabori M, Niiya Y, et al. Experience of (123)I-iomazenil SPECT study for crossed cerebellocerebral diaschisis: report of two cases. Clin Neurol Neurosurg. 2012;114(9):1274-1276.

[4] Baron JC, Bousser MG, Comar D, et al. "Crossed cerebellar diaschisis" in human supratentorial brain infarction. Trans Am Neurol Assoc. 1981;105:459-461.

[5] Agrawal KL, Mittal BR, Bhattacharya A, et al. Crossed cerebellar diaschisis on F-18 FDG PET/CT. Indian J Nucl Med. 2011;26(2):102-103.

[6] Lin DD, Kleinman JT, Wityk RJ, et al. Crossed cerebellar diaschisis in acute stroke detected by dynamic susceptibility contrast MR perfusion imaging. AJNR Am J Neuroradiol. 2009;30(4):710-715.

[7] Yamada H, Koshimoto Y, Sadato N, et al. Crossed cerebellar diaschisis: assessment with dynamic susceptibility contrast MR imaging. Radiology. 1999;210(2):558-562.

[8] Evans AL, Widjaja E, Connolly DJ, et al. Cerebral perfusion abnormalities in children with Sturge-Weber syndrome shown by dynamic contrast bolus magnetic resonance perfusion imaging. Pediatrics. 2006;117(6):2119-2125.

[9] Huang L, Wang XH, Liu SR. The application of DW I and ADC mapping in acute cerebral infarction and basis of pathophysiology. Zhongguo Bingli Shengli Zazhi. 2002; 18(6):687-689.

[10] Zhang QJ, Yang JL, Guo YM, et al. ADC values in healthy adult brain: measurement and influencing factors. Shiyong Fangshe Xue Zazhi. 2008;24(7):870-873, 876.

[11] Lambregts DM, Maas M, Riedl RG, et al. Value of ADC measurements for nodal staging after chemoradiation in locally advanced rectal cancer-a per lesion validation study. Eur Radiol. 2011;21(2):265-273.

[12] Zhong GX, Zhu WZ, Wang W, et al. Quantitative evaluation of ischemic penumbra of hyperacute cerebral infarction with diffusion weighted imaging, perfusion weighted imaging and mr spectroscopy. Fangshe Xue Shijian. 2006;21(6):541-545.

[13] Lim KS, Tan CH. Diffusion-weighted MRI of adult male pelvic cancers. Clin Radiol. 2012;67(9):899-908.

[14] Liu GH, Li LS, Zhou Q, et al. Diffusion and perfusion MR imaging of acute cerebral ischemia with reperfusion: a experiment in rats. Zhongguo Yixue Yingxiang Xue Zazhi. 2007;5(6):428-432.

[15] Qiu QD, Xu JJ, Liu X, et al. Evaluation of DWI combined with ADC mapping in the diagnosis of acute cerebral infarction. Fangashe Xue Shijian. 2006;21(2):126-129.

[16] Lin W, Lee JM, Lee YZ, et al. Temporal relationship between apparent diffusion coefficient and absolute measurements of cerebral blood flow in acute stroke patients. Stroke. 2003;34(1):64-70.

[17] Kong XQ, Liu DX, Jiang L, et al. Time course of changes in signal intensity and apparent diffusion coefficient on diffusion-weighted images in cerebral infarction. Zhonghua Fangshe Xue Zazhi. 2000;34(5):325-329.

[18] Han HB, Wang J, Xie JX, et al. The differential diagnosis of hyperintensity lesions on high diffusion sensitive gradient diffusion-weighted imaging. Zhonghua Fangshe Xue Zazhi. 2002;36(9):812-816.

[19] Wang YJ, Yao QL, Fang F, et al. A study of ischemic penumbra by perfusion and diffusion-weighted imaging at high-field MRI (7.0 T). Zhonghua Yi Xue Za Zhi. 2010; 90(25):1773-1777.

[20] Cvoro V, Marshall I, Armitage PA, et al. MR diffusion and perfusion parameters: relationship to metabolites in acute ischaemic stroke. J Neurol Neurosurg Psychiatry. 2010; 81(2):185-191.

[21] Gonen KA, Simsek MM. Diffusion weighted imaging and estimation of prognosis using apparent diffusion coefficient measurements in ischemic stroke. Eur J Radiol. 2010;76(2):157-161.

[22] Holmes WM, Lopez-Gonzalez MR, Gallagher L, et al. Novel MRI detection of the ischemic penumbra: direct assessment of metabolic integrity. NMR Biomed. 2012; 25(2):295-304.

[23] Ma L, Gao PY, Hu QM, et al. Effect of baseline magnetic resonance imaging (MRI) apparent diffusion coefficient lesion volume on functional outcome in ischemic stroke. Neurol Res. 2011;33(5):494-502.

[24] Huang YC, Weng HH, Tsai YT, et al. Periictal magnetic resonance imaging in status epilepticus. Epilepsy Res. 2009;86(1):72-81.

[25] Samaniego EA, Stuckert E, Fischbein N, et al. Crossed cerebellar diaschisis in status epilepticus. Neurocrit Care. 2010;12(1):88-90.
[26] Poretti A, Boltshauser E. Crossed cerebro-cerebellar diaschisis. Neuropediatrics. 2012;43(2):53-54.
[27] Kamouchi M, Fujishima M, Saku Y, et al. Crossed cerebellar hypoperfusion in hyperacute ischemic stroke. J Neurol Sci. 2004;225(1-2):65-69.
[28] Devor A, Ulbert I, Dunn AK, et al. Coupling of the cortical hemodynamic response to cortical and thalamic neuronal activity. Proc Natl Acad Sci U S A. 2005;102(10):3822-3827.
[29] Le Bihan D, Breton E, Lallemand D, et al. MR imaging of intravoxel incoherent motions: application to diffusion and perfusion in neurologic disorders. Radiology. 1986;161(2):401-407.
[30] Chu B, Shao GF, Bao SR, et al. The alteration of rCBF in the remote area after focal cerebral ischemia of rat. Suzhou Daxue Xuebao: Yixue Ban. 2003;23(2):152-153.
[31] Finger S, Koehler PJ, Jagella C. The Monakow concept of diaschisis: origins and perspectives. Arch Neurol. 2004;61(2):283-288.
[32] Kempinsky WH. Vascular and neuronal factors in diaschisis with focal cerebral ischemia. Res Publ Assoc Res Nerv Ment Dis. 1966;41:92-115.
[33] Slater R, Reivich M, Goldberg H, et al. Diaschisis with cerebral infarction. Stroke. 1977;8(6):684-690.
[34] Lenzi GL, Frackowiak RS, Jones T. Cerebral oxygen metabolism and blood flow in human cerebral ischemic infarction. J Cereb Blood Flow Metab. 1982;2(3):321-335.
[35] Wise RJ, Rhodes CG, Gibbs JM, et al. Disturbance of oxidative metabolism of glucose in recent human cerebral infarcts. Ann Neurol. 1983;14(6):627-637.
[36] Nagasawa H, Kogure K. Exo-focal postischemic neuronal death in the rat brain. Brain Res. 1990;524(2):196-202.
[37] Izumi Y, Haida M, Hata T, et al. Distribution of brain oedema in the contralateral hemisphere after cerebral infarction: repeated MRI measurement in the rat. J Clin Neurosci. 2002;9(3):289-293.
[38] Wang LL, Cheng JL, Zhang Y, et al. A perfusion-weighted MRI analysis crossed cerebellar diaschisis. Zhengzhou Daxue Xuebao: Yixue Ban. 2011;46(2):308-310.
[39] Zhao SS, Cheng JL, Bao J, et al. Perfusion weighted imaging assessment of the relationship between volume of cerebral infarction and crossed-cerebellar diaschisis in different stages of cerebral infarction. Fangshe Xue Zazhi. 2012;27(9):951-953.
[40] Madai VI, Altaner A, Stengl KL, et al. Crossed cerebellar diaschisis after stroke: can perfusion-weighted MRI show functional inactivation? J Cereb Blood Flow Metab. 2011;31(6):1493-1500.
[41] Jeon YW, Kim SH, Lee JY, et al. Dynamic CT perfusion imaging for the detection of crossed cerebellar diaschisis in acute ischemic stroke. Korean J Radiol. 2012;13(1):12-19.
[42] The Ministry of Science and Technology of the People's Republic of China. Guidance Suggestions for the Care and Use of Laboratory Animals. 2006-09-30.
[43] Longa EZ, Weinstein PR, Carlson S, et al. Reversible middle cerebral artery occlusion without craniectomy in rats. Stroke. 1989;20(1):84-91.

(Reviewed by Dean J, Robens J, Sun XJ, Huang LA)
(Edited by Yu J, Yang Y, Li CH, Song LP, Liu WJ, Zhao M)